ARTICLE

Journal of Materials Chemistry
www.rsc.org/materials

Porosity of core–shell nanoparticles†

V. Suryanarayanan, A. Sreekumaran Nair, Renjis T. Tom and T. Pradeep*

Department of Chemistry and Sophisticated Analytical Instrument Facility, Indian Institute of Technology Madras, Chennai 600 036, India. E-mail: pradeep@iitm.ac.in; Fax: ++91-44-2257 0509

Received 23rd March 2004, Accepted 2nd June 2004
First published as an Advance Article on the web 20th July 2004

The porosity of titania and zirconia covered Ag and Au nanoparticles has been investigated using the metal core reactivity as a probe. The presence of pores was confirmed by a newly discovered reaction between halocarbons and core–shell nanoparticles, in which the core gets converted into ions, which are leached out through the shell. Halocarbons having different alkyl chain lengths react with metal cores at different rates due to the differences in the accessibility of the core. It is also observed that the electrochemical accessibility of the core can be reduced by blocking the pores by adsorbates such as *cis*-dithiocyanato-bis(2,2′-bipyridyl-4,4′-dicarboxylic acid)ruthenium(II) dye (popularly called N3 dye). With the adsorbed dye molecules on the oxide shell, metal cores are stable for extended periods of time even after the addition of halocarbons. The porosity of the $Au@SiO_2$ system, in which a silica shell is formed over the metal clusters through monolayers, has also been studied. Our studies show that the porosity of different kinds of shells is largely similar, allowing molecular and ion penetration.

Introduction

Core–shell nanoparticles, especially those with oxide shells, are interesting from a number of perspectives.[1–4] The shells offer protection to the cores as well as introduce new properties to the hybrid structures.[5] Silica protected gold and silver nanoparticles have been used for a number of investigations in the recent past.[6–9] Recently, variation in the melting point of these particles has been investigated by Meisel *et al.*[10] While the chemistry of the core–shell structure is interesting, leaching out the metal cores can produce newer chemical systems.[11–13] Core–shell systems are also attractive in certain other areas because of the presence of inert barriers around nanoparticles. One area of application is in biology where toxic cores such as CdSe are delivered *in vivo*.[14–16] Specific electronic properties make it possible to use these 'coated' systems in dye sensitized solar cells.[17] The use of semiconducting nanophase materials such as CdS in industrial applications requires them to be coated with inert shells to give them long-term stability.[18] One of the critical issues concerning the properties of core–shell systems, especially in solution or at a liquid–solid interface, is their porosity. Chemical and electrochemical accessibility of the core depends on the porosity of the shells.[11,12]

An important shell forming material is TiO_2, which offers wide-ranging properties.[17] Nanophase TiO_2 is often prepared by the selective hydrolysis of alkoxide precursors. Various post-synthesis approaches exist to improve the quality of the nanophase material; most of this work has been done in relation to dye-sensitized solar cells.[17] We have been interested in core–shell structures especially because the oxide cover can protect the cores from photo-fragmentation in optical limiting applications of metal clusters.[19] The shells themselves are useful as ceramic cages, in which a variety of molecular species may be trapped. It is in this context that we decided to pursue a detailed investigation into the porosity of TiO_2 and ZrO_2 protected Au and Ag core–shell nanoparticles. We have shown that TiO_2 and ZrO_2 shells can be formed on Au and Ag nanoparticles by a single step procedure,[20] the TiO_2 shell chemistry has already been demonstrated by Liz-Marzan and colleagues.[13] The particles are extremely stable, and they can be separated, cleaned and re-suspended.[20] Studies suggest that the shells completely protect the particles and the shell thickness can be uniformly varied by simple procedures.[6,20] ZrO_2 coated nanoparticles have been made by the monolayer route as well.[21]

In this paper, we describe an investigation into the porosity of two types of core–shell nanosystems made with two different routes. Most of the studies were on particles prepared by the one-step method in which the precursor and the metal ions are taken in the same solution, and are referred to below as type I particles ($Au/Ag@ZrO_2$ and $Au/Ag@TiO_2$). While the metal ions underwent reduction by dimethyl formamide (DMF), the oxide precursor hydrolyzed and formed a coating on the metal.[5,22–24] The chemistry is similar for TiO_2 and ZrO_2 shells and we may switch between these two systems in later sections. The results are supported by studies on other kinds of particles, in which a silica shell is formed over the metal clusters through monolayers,[6] and are referred to below as type II particles ($Au@SiO_2$). Investigations used principally two tools, namely UV-visible spectroscopy and cyclic voltammetry, both sensitive to the changes to the core while molecules (which can react with metal cores) go through the shells. The particles used here were characterized completely by a variety of techniques earlier[20,21] and we will not be elaborating on these measurements. We have also shown that core–shell systems offer additional flexibility by functionalizing the shells with monolayers.[25] We have shown that metal nanoparticles react with halocarbons[26] and this reactivity can be applied to core–shell systems to remove metal cores forming hollow shells.[11] The present study is based on these earlier reports and extends the halocarbon chemistry of nanoparticles using several molecules with the objective of probing the porosity of the shells.

It is important to contrast the shells in core–shell materials from the bulk TiO_2, ZrO_2 and SiO_2 materials prepared by the sol–gel processes[27] which have been investigated in great detail

† Electronic supplementary information (ESI) available: UV-visible spectrum showing the emergence of a peak corresponding to $AuCl_3$ in the reaction between $Au@TiO_2$ and benzyl chloride, time dependent CV of $Ag@ZrO_2$ on Pt electrode showing the effect of addition of 100 μl of 1-bromohexane and 1-bromododecane, CV of the free N3 dye and its variation upon interaction with $Au@TiO_2$, as well as time dependent CV of $Au@SiO_2$ nanoparticles having shell thickness of 60–80 nm upon reaction with benzyl chloride (4 pages). See http://www.rsc.org/suppdata/jm/b4/b404408h/

DOI: 10.1039/b404408h

from the perspective of catalysis. In fact porosity is an important aspect in the chemistry of such systems. The materials investigated here are distinctly different. These are made in solution and no high temperature treatment is done unlike the sol–gel derived materials. As a result they form stable solutions for extended periods. It may be added that only very little is known about the porosity of these new materials.

Experimental

$HAuCl_4 \cdot 3H_2O$ and $AgNO_3$ were purchased from CDH chemicals. Titanium(IV) isopropoxide $Ti[OCH(CH_3)_2]_4$ and zirconium(IV) propoxide were from Aldrich. *cis*-Dithiocyanato-bis(2,2′-bipyridyl-4,4′-dicarboxylic acid)ruthenium(II) dye (N3 dye, a well-known adsorbent forming monolayer) was synthesized as per the literature procedure.[28] Aminopropyl trimethoxy silane (APS) and tetraethoxysilane were obtained from Aldrich. All the solvents used in the synthesis were from local sources and were distilled prior to use. The chemicals were of 99.9% or higher rated purity. The purity was not independently checked except by UV-visible absorption spectroscopy, wherever necessary. The core–shell particles were synthesized by two methods. In one method (leading to type I particles), zirconia or titania covered silver or gold nanoparticles were prepared by one-pot synthesis. In the procedure, a solution containing equimolar (20 mM) amounts of $Ti[OCH(CH_3)_2]_4$ (or zirconium(IV) propoxide) and acetyl acetone in 2-propanol was prepared. A clear solution was formed upon mild sonication. Another solution of 9 mM $AgNO_3$ (or $HAuCl_4 \cdot 3H_2O$) and 14 M H_2O in DMF was prepared. 40 ml of the first solution and 20 ml of the second solution were mixed and stirred for about 10 minutes. The mixture was then transferred to a heating mantle and refluxed for 45 minutes. The solution became wine red in the case of gold and greenish-black in the case of silver. This solution consisted of core shell particles of $\sim$30–60 nm core diameter and $\sim$3 nm shell thickness.[20] The color change during synthesis was abrupt in the case of Au and more gradual in the case of Ag. Further refluxing of the solution led to the formation of a precipitate, which could be dispersed by sonication. The colloidal material was precipitated by the addition of toluene.[20] The precipitate was washed repeatedly with toluene and it was re-dispersed in 2-propanol. Dry powders were not re-dispersible. The solutions are stable for over two months. Ag particles were better dispersible than Au; the latter showed aggregation with the passage of time. In all cases, increasing the precursor concentration while keeping the reaction time constant varies the shell thickness.[20]

In the second method (leading to type II particles), the core–shell particles of $Au@SiO_2$ were prepared by the method reported by Liz-Marzan *et al.*[6] 100 ml of 5×10^{-4} M gold sol was prepared by the versatile sodium citrate reduction method.[29] The average particle diameter was 15 nm. 0.5 ml of 1 mM freshly prepared aqueous solution of aminopropyl trimethoxy silane (APS) was added under vigorous magnetic stirring and the mixture was kept for 15 minutes for complete complexation of amino groups with the gold surface. About 4 ml of active silica (by bringing the pH of 0.54 wt% solution of sodium silicate solution to 10–11 by progressively adding cation exchange resin, Dualite, 225-Na 14–52 mesh from BDH Chemical, converted into the acid form by repeated washing with acid and water) was then added to the gold sol, again under vigorous magnetic stirring. The resulting mixture was then allowed to stand for one day to get a silica shell of 2–4 nm thickness. The shell thickness was increased further by transferring the colloidal solution into ethanol (1:4 by volume) and 0.3 ml of tetraethoxysilane and 2 ml ammonium hydroxide were added and allowed to stand for 12 h under mild stirring. In this way, the shell thickness was increased to 80 nm.[6]

The samples were characterized thoroughly using UV-visible spectroscopy, transmission electron microscopy (TEM), X-ray diffraction (XRD), infrared spectroscopy (IR) and cyclic voltammetry (CV).[20] UV-visible spectra were measured with Varian Cary 5 UV/VIS/NIR and Perkin Elmer Lambda 25 spectrometers. Transmission electron microscopic images were taken from a JEOL 3010 high-resolution instrument working at 300 KeV energy. X-Ray diffraction measurements were taken with a Shimadzu XD-D1 diffractometer with Cu Kα radiation (30 kV, 20 mA). Infrared spectra were measured using a Perkin Elmer Spectrum One spectrometer. Cyclic voltammetry data were obtained with an Electrochemical Analyzer (CH Instruments Model 600A) in a standard three-electrode cell comprising a Pt disk (area = 0.8 mm^2) as working electrode, a platinum foil as counter electrode and Ag/AgCl as the reference electrode. Voltammetry was performed at various scan rates in acetonitrile containing 0.1 M tetrabutylammonium hexafluorophosphate (TBAHFP) as supporting electrolyte in which the colloidal solutions were dispersed. In order to prevent memory effects on the Pt electrode surface, it was cleaned prior to each experiment. In the studies mentioned here, the concentration of the nanoparticle solution is not specified, as there is a distribution in particle sizes.

Results and discussion

We shall first discuss the results on type I particles, followed by those on type II particles. Although the former are more recent, detailed studies on several properties of both these systems exist in the literature and therefore we shall confine ourselves to the porosity studies only. We shall not discuss the characterization aspects of the particles, except those evidently needed for this study.

We have found that the colloidal solutions of core–shell nanoparticles exhibit interesting reactivity upon addition of halocarbons.[11] These reactions result in the selective leaching of the metal core as metal halides resulting in the formation of metal oxide nanobubbles.[11] AgCl precipitates completely while $AuCl_3$ can be extracted from the solution and details of these reactions have been investigated.[26] The metal ions are leached out completely through the shells as a result of reactions occurring with metal cores. The solution after removal of the core was imaged by transmission electron microscopy. In the case of ZrO_2 protected clusters, stable nanobubbles were observed.[11] The bubbles obtained from TiO_2 protected clusters were not stable under the electron beam. The existence of bubbles suggests that the shell is permeable for molecules and ions. This shows that the porosity of core–shell systems can be investigated using halocarbon reactivity as a probe.

The time dependent UV-visible spectra clearly show the reaction between metal core and halocarbons. The reactions are faster with Ag than with Au. In Fig. 1A we show the time dependent UV-visible spectra upon the addition of 100 μl of benzyl chloride into 4 ml of the $Au@TiO_2$ colloidal solution. Trace a is the absorption spectrum of pure $Au@TiO_2$. Trace b was recorded 20 minutes after the addition of benzyl chloride. The reaction is slow, the plasmon band profile changes in shape with time and a two-peak structure develops. The subsequent traces (c–l) were taken at intervals of 20 minutes. The shift in the plasmon is due to the adsorption of benzyl chloride onto the gold surface and the resultant aggregation of the particles. The solution turns blue and if it is left undisturbed, the bluish material precipitates (which could be re-dispersed by sonication). Upon stirring the solution, the reaction goes to completion within 10 h, indicating the complete conversion of gold to Au^{3+} (see ESI 1,† for the absorption spectrum of Au^{3+}). At this stage the plasmon disappeared completely (trace z). An identical reaction sequence was observed for $Au@ZrO_2$ also. Fig. 1B shows the UV-visible spectra of the time dependent

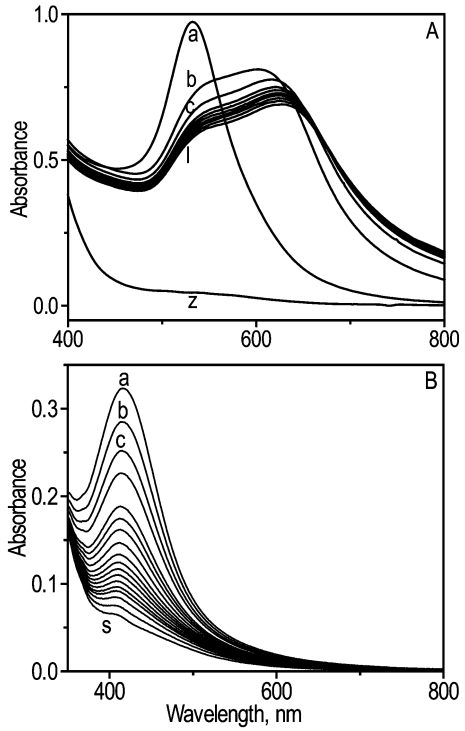

Fig. 1 Time dependent UV-visible spectra of (A) Au@TiO_2 and (B) Ag@TiO_2 showing the effect of addition of 100 μl of $PhCH_2Cl$. In Fig. 1A, trace a is the absorption spectrum of pure Au@TiO_2. Trace b was recorded 20 minutes after the addition of 100 μl of benzyl chloride. Subsequent traces (c–l) were recorded at intervals of 20 minutes. The plasmon disappears completely within 10 h with stirring (trace z). In B, a is the absorption spectrum of pure Ag@TiO_2, b is taken immediately after the addition of the same amount of benzyl chloride. Traces (c–s) were taken at an interval of 10 minutes after the addition of benzyl chloride. Note that the reduction in plasmon is continuous and it disappears completely after 200 minutes.

reaction of benzyl chloride with Ag@TiO_2. The traces were recorded at intervals of 10 minutes. The reaction is fast and the intensity of the plasmon decreases continuously with time when compared to gold and after 200 minutes, the plasmon completely disappears. At this point the solution turns gray-white and upon standing, a precipitate separates out, which was characterized by powder X-ray diffraction to be composed of AgCl. An identical reaction sequence occurs with Ag@ZrO_2 as well. Unlike Au, the halocarbons directly react at the Ag nanoparticles' surface and the dielectric constant of silver does not change much and hence its plasmon absorption feature does not shift during the halocarbon reaction. The results presented above suggest that the oxide shells are porous for molecular transport.

To study the nature of the pores in the nano shells, three different halocarbons having different chain lengths were taken and their reactivity with the metal core was investigated by cyclic voltammetry. Core–shell nanomaterials are electroactive in their solution phase and they show well-defined redox peaks in cyclic voltammetry (CV). The electron transfer properties of the core can manifest only through the pores in the case of core–shell nanomaterials. The three different halocarbons taken are bromoform, 1-bromohexane and 1-bromododecane and their reactivity with ZrO_2 protected Ag clusters was studied. A typical time dependent CV of Ag@ZrO_2 with 100 μl of bromoform on Pt electrode in CH_3CN containing 0.1 M tetrabutylammonium hexafluorophosphate (TBAHFP) at a sweep rate of 300 mV s^{-1} at 5 minute intervals is shown in Fig. 2. Ag@ZrO_2 shows a characteristic anodic peak at 0.310 V and a cathodic peak at 0.120 V in the solution phase containing 0.1 M TBAHFP/CH_3CN on the Pt electrode surface[11,30,31] (curve a). The redox

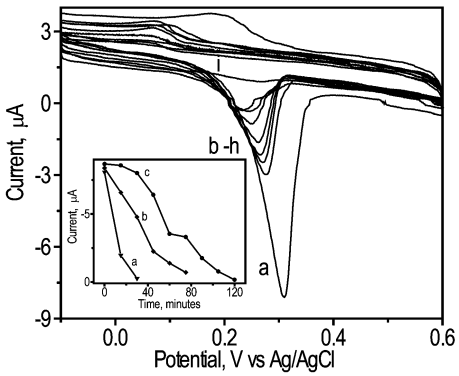

Fig. 2 Time dependent CV of Ag@ZrO_2 on Pt electrode showing the effect of addition of 100 μl of bromoform. The voltammetric curve a is that of pure Ag@ZrO_2, traces from (b–h) were taken at time intervals of 5 minutes just after the addition of bromoform. All data were collected at a sweep rate of 300 mV s^{-1}. The medium is CH_3CN containing 0.1 M tetrabutylammonium hexafluorophosphate (TBAHFP). Inset: Plot of anodic peak current of Ag@ZrO_2 *vs.* time depicting the reactivity with different bromocarbons, a) bromoform, b) 1-bromohexane and c) 1-bromododecane under identical conditions.

couple is centered at $E_{1/2} = 0.215$ V *vs.* Ag/AgCl with a peak separation, ΔE_p, of 0.190 V for the anodic peak (curve a). The quasi-reversible peaks corresponding to the oxidation and reduction of Ag clusters can be represented as,

$$Ag_n \rightarrow Ag_n^+ + e \quad (1)$$

For dodecanethiol capped silver clusters, the anodic peak is around 0.242 V *vs.* Ag/AgCl with ΔE_p of 0.229 V,[32] and the peak potential for Ag@ZrO_2 is towards a more positive value.

After the addition of the reactant, the characteristic peak current due to the Ag/Ag^+ redox couple decreases (curve b–h), which finally becomes flat at the end of 35 minutes (curve i), confirming the complete leaching of Ag as AgBr. Similar reactions were observed with different time scales for 1-bromohexane and 1-bromododecane in cyclic voltammetry experiments (ESI 2†). The inset shows a plot of the decrease in anodic peak current of Ag@ZrO_2 *vs.* time for the reaction with bromoform (a), 1-bromohexane (b) and 1-bromododecane (c). From the plots, it is clear that the reactivity of bromocarbons with the Ag core decreases with increase in their chain length. The difference in their reactivity with metal cores can be attributed to the decreasing ability to penetrate through the shell depending upon their size. Small molecules ($CHBr_3$) penetrate through the pores more easily than the larger ones.

Having established the porosity of different nano shells, we wanted to check whether the reaction with the cores could be prevented partially or completely by blocking the pores or the surface of the oxide shell. Among the four systems we have, Au@TiO_2 was chosen for this study as TiO_2 films are frequently used in dye sensitized solar cells. In Fig. 3A, we show the changes in the absorption spectrum of Au@TiO_2 upon exposure to varying concentrations of N3 dye in 1-propanol. The traces a and b in Fig. 3A correspond to the absorption spectra of the dye and pure Au@TiO_2, respectively. Upon addition of the dye, the absorption spectrum progressively changes; the coverage of the TiO_2 surface with the dye is manifested by the emergence of a peak at 400 nm.

When the dye concentration was increased beyond 22.3×10^{-6} M (curve h), the spectrum resembled more like the dye, indicating saturation coverage and thereafter the dye coated particles precipitated. The precipitation was accelerated by centrifugation and the material was re-dispersed in 3 ml of acetonitrile. To this 100 μl of benzyl chloride was added and absorption spectra were monitored as a function of time. Time dependent UV-visible spectra at an interval of 30 minutes are

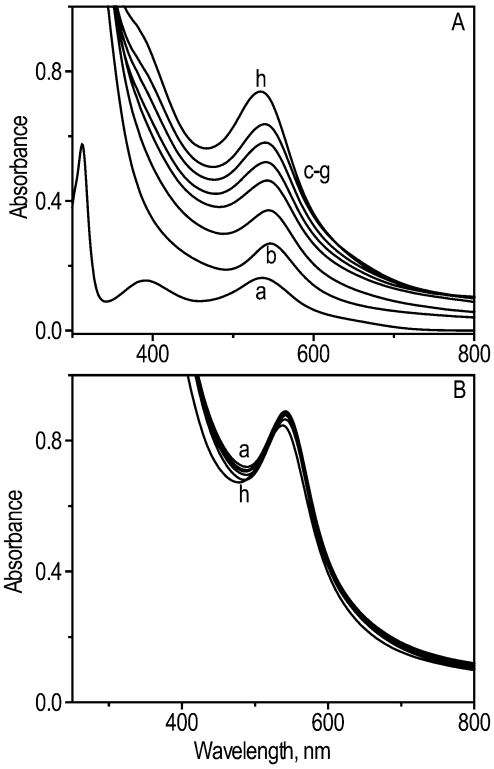

Fig. 3 A: UV-visible spectra showing the effect of adsorption of N3 dye on Au@TiO_2, a and b show the absorption spectra of dye and Au@TiO_2 respectively, c to h show the effect of adding different concentrations of N3 dye to Au@TiO_2, c = 4.75×10^{-6}, d = 9.3×10^{-6}, e = 13.8×10^{-6}, f = 18.1×10^{-6}, g = 22.3×10^{-6} and h = 25.4×10^{-6} (M). B: Time dependent UV-visible spectra of the reaction between dye adsorbed Au@TiO_2 and 100 μl of $PhCH_2Cl$ (a–h) at intervals of 30 minutes.

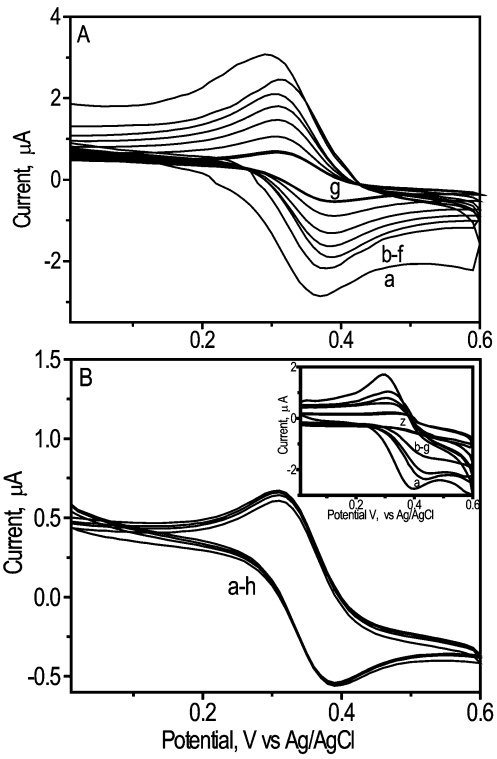

Fig. 4 A: CV of Au@TiO_2 showing the effect of addition of different concentrations of N3 dye at a constant sweep rate of 300 mV s^{-1}. Curve a shows the CV of the bare substrate and b to g show the effect of adding different concentrations of dye into Au@TiO_2 (concentrations in M); b = 4.75×10^{-6}, *c* = 9.3×10^{-6}, d = 13.8×10^{-6}, e = 18.1×10^{-6}, f = 22.3×10^{-6}, g = 25.4×10^{-6}. B: Time dependent CV of dye coated Au@TiO_2 showing the effect of addition of 100 μl of $PhCH_2Cl$ (a–h). The traces were recorded at time intervals of 30 minutes. The sweep rate was 300 mV s^{-1}. Inset shows the time dependent CV of Au@TiO_2 (a) with 100 μl of benzyl chloride in the absence of dye at time intervals of 30 minutes (b–g) at the same sweep rate. Curve z was taken at 10 h of reaction.

shown in Fig. 3B. UV-visible spectra showed that the shell is resistant to molecular penetration because of the blocking of its pores, after the adsorption of a monolayer of dye molecules (N3 dye adsorption on nanoTiO_2 leading to a monolayer is known[17]).

The porous nature of TiO_2 nanoshells has been studied by CV using $[Fe(CN)_6]^{3-}$ as the probe ion.[13] Cyclic voltammograms indicate that coverage of Au@TiO_2 completely passivates the electrode surface and blocks the redox property of $[Fe(CN)_6]^{3-}$ whereas for TiO_2 nanoshells (*i.e.* without the core), a strong current is noticed in which redox accessibility of $[Fe(CN)_6]^{3-}$ towards the electrode surface is achieved through the pores of the TiO_2 shell.[13] Using these inputs we studied the effect of dye adsorption on the surface of the TiO_2 shell. In Fig. 4A, a series of superimposed cyclic voltammograms obtained by the addition of N3 dye to Au@TiO_2 metal clusters are shown at a constant sweep rate of 300 mV s^{-1}. Curve a shows the cyclic voltammogram of pure Au@TiO_2. Au@TiO_2 shows a characteristic reversible redox couple centered at $E_{1/2}$ = 0.330 V and an anodic peak at 0.370 V with a peak separation, ΔE_p, of 0.064 V *vs.* Ag/AgCl.[30] The sharp and symmetrical anodic peak at this potential suggests one electron transfer reaction of the gold nanoclusters[30] ($Au_n \rightarrow Au_n^+ + e$). As the dye is added in different concentrations, the peak current decreases gradually (curves b–f) and beyond a concentration of 22.3×10^{-6} M, no change is observed in the CV indicating that surface coverage has attained the saturation value (curve g). There was a slight shift in the peak potential upon the first addition of the dye, but subsequent additions did not change the potential anymore. The voltammograms do not change with time and it is clear that the adsorption of dye occurred almost instantaneously.

Variation in the cyclic voltammograms upon addition of 100 μl of benzyl chloride to the above system (dye coated Au@TiO_2) is shown in Fig. 4B. Cyclic voltammograms in conjunction with optical absorption spectroscopy suggest that the reaction has been slowed down considerably, which shows the effective adsorption of dye on the pores or surface of the oxide shell. A set of CV traces in the absence of the dye under the same conditions is shown in the inset for comparison. With the addition of 100 μl of benzyl chloride, both the cathodic and anodic currents are found to decrease with time (curve b–g) and finally attain the background current of Pt in CH_3CN containing TBAHFP (curve z). The decrease in peak current is due to the removal of electro-active Au nanoparticles from the electrolyte system by the reaction with benzyl chloride. There is also some shift in the peak potential towards the cathodic side, which is random unlike that of the same reaction with Ag@ZrO_2 nanoparticles[11] and may be due to ohmic drop as a result of blocking.

The electrochemical reaction rate for the core removal of the above system before and after the adsorption of dye molecule was calculated from the cathodic peak current. The tunneling of electrons through the shell is disregarded since it is less significant. The first order rate constants (*k*) before and after dye adsorption are 2.6×10^{-3} and 1.7×10^{-3} s^{-1}, respectively for the Au@TiO_2 system (from UV-visible studies, the calculated rate constant values are 3.0×10^{-3} and 1.4×10^{-3} s^{-1} respectively). This confirms that the rate of halocarbon reaction with Au cores is considerably reduced after the adsorption of dye molecules.

Voltammograms were also recorded by scanning the potential from −1.5 V to 0.5 V in order to characterize N3 dye molecules during the course of their adsorption on Au@TiO_2. Voltammetry in this potential window reveals one reversible redox couple attributed to Ru(II/III). In the free dye, this couple is observed at −0.99 V (ESI 3†). However, for the dye adsorbed on the shell, the redox potential is slightly shifted to −1.04 V. This shift of potential can be attributed to the strong interaction/adsorption of the dye molecule on the surface of the oxide shell and/or the pores. With further addition of dye to the nanoparticle solution, the peak current increases gradually and attains a saturation value. This can be observed clearly from the plot of peak current *vs.* concentration of dye added (inset of ESI 3B†). In the cyclic voltammogram of the adsorbed dye molecule, one pre-wave is noted at −0.52 V. However, at a slower scan rate, this pre-wave does not appear and hence it is characterized as the adsorption wave (inset of ESI 3A†).

The effect of shell thickness on the reactivity of benzyl chloride was investigated with type II (Au@SiO_2) particles. The size of the shell can be controlled with precision in this case by varying synthetic parameters.[6] Fig. 5 shows the time dependent CV showing the effect of addition of 100 μl of benzyl chloride to Au@SiO_2 particles having a shell thickness of 4 nm. Curve a shows the CV in the absence of reactant and the other curves are in its presence. The traces were recorded at intervals of 15 minutes. Similar to the Au@TiO_2 system, Au@SiO_2 with a shell thickness of 4 nm also shows reversible redox peaks on Pt electrode under identical experimental conditions (Fig. 5 curve a). The anodic peak potential is at 0.300 V and the cathodic peak is at 0.210 V suggesting one electron transfer reaction of gold nano clusters (bare gold electrode has an oxidation potential of 1.2 V *vs.* NHE in 1.0 M sulfuric acid[32]). With the addition of benzyl chloride, however, the peak current decreases (curves b–i) and at 10 hours and 20 minutes, the reaction is complete indicating complete removal of Au nanoparticles (curve j). However, for Au@SiO_2 nanoclusters having larger shell thickness (60–80 nm, prepared by changing preparative conditions[6]) it is observed that both the characteristic peak potentials (cathodic and anodic) got shifted towards a more positive value, which shows that the redox accessibility of Au_n/Au_n^+ is reduced with increasing shell thickness. With the addition of benzyl chloride, the peak intensity was found to decrease and becomes the background current only after 14 hours and 25 minutes (ESI 4†). A plot of normalized I_p *vs.* time for low (trace a) and high (trace b) shell thicknesses shows the difference in reaction rates. The slope of the curve is larger

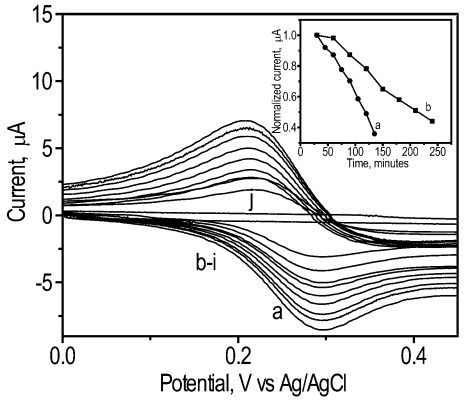

Fig. 5 Time dependent CV of Au@SiO_2 nanoparticles having shell thickness of 4 nm upon reaction with 100 μl of benzyl chloride. Curve a shows CV in the absence of the reactant and others in its presence at a sweep rate of 300 mV s^{-1}. The traces were recorded at intervals of 15 minutes. Complete quenching of the redox peak is found to occur after 10 hours and 20 minutes. Inset shows the plot of peak current *vs.* time showing the quenching phenomena for (a) low and (b) high thickness (the time for final quenching is not shown in the plot).

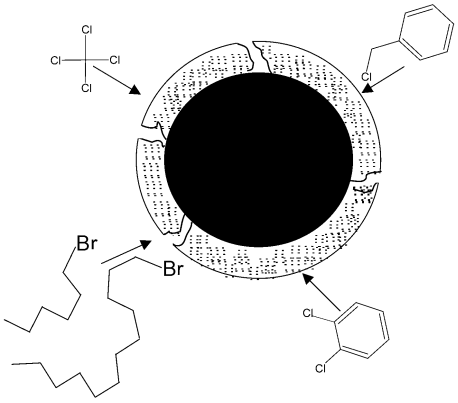

Fig. 6 Schematic representation of a core–shell particle. The shell largely covers the core, but has interconnected channels, which can take molecules such as CCl_4, $CHBr_3$, $C_6H_5CH_2Cl$, 1-bromohexane and 1-bromododecane into the core where they react with the cores. The alkyl bromides are shown to have *gauche* defects, as expected in the solution state.

for the smaller shell thickness as expected. As the molecular dimension of benzylchloride is ∼4.2 Å, the pore sizes should be of the order of several Å. Several of the molecules shown to exhibit reactivity with the core such as CCl_4, $CHCl_3$ and $CHBr_3$ are also of similar dimension. As the N3 dye (size ∼ 1.6 nm) molecules partially block the pores and thereby slow down the halocarbon reaction with the metal core, the pore sizes should be definitely less than this value.

Summary and conclusions

Metal cores in core–shell nanoparticles are accessible by ions so as to effect electron transfer reactions. The cores can be accessed by neutral molecules also. Reactions of halocarbons with core–shell particles lead to the selective leaching of cores resulting in metal oxide nanobubbles. Experiments reveal that the electrochemical accessibility of the core can be reduced by the adsorption of dyes on the pores or on the shell surface. Also, increasing the thickness of the shell reduces the redox accessibility of the core, but beyond a shell thickness of 80 nm, the particles are not re-dispersible and investigations became difficult. The pores can be partially or completely blocked by molecules as large as the N3 dye. Results indicate that the pore dimension is of the order of several Å. A similar situation is suggested to exist in nanoTiO_2 films used for dye sensitized solar cells. On the basis of these experiments, we suggest that the structure of the core–shell particles is likely to be similar to that depicted in Fig. 6. Pores of this kind may not be observable in TEM, as a two-dimensional projection would only show complete shells.

Acknowledgements

T. P. acknowledges the financial support from Ministry of Information Technology, Department of Science and Technology of Government of India (Nanoscience initiative) and Space Technology Cell of Indian Institute of Technology Madras. V. S. and R. T. T. thank the Council of Scientific and Industrial Research for the award of a research associateship and a junior research fellowship, respectively.

References

1 N. Kakuta, K. H. Park, M. F. Finlayson, A. Veno, A. J. Bard, A. Campion, M. A. Fox, S. E. Webber and J. M. White, *J. Phys. Chem.*, 1985, **89**, 3828.
2 C. Nasr, S. Hotchandani, W. Y. Kim, R. H. Schmehl and P. V. Kamat, *J. Phys. Chem. B*, 1997, **101**, 7480.
3 S. S. Davis, *Trends. Biotechnol.*, 1997, **15**, 217.

4 S. Tomilson, P. W. Taylor and J. P. Luzio, *Biochemistry*, 1989, **28**, 1989.
5 I. Pastoriza-Santos, D. S. Koktysh, A. A. Mamedov, M. Giersig, N. A. Kotov and L. M. Liz-Marzan, *Langmuir*, 2000, **16**, 2731.
6 T. Ung, L. M. Liz-Marzan and P. Mulvaney, *J. Phys. Chem. B*, 1999, **103**, 6770.
7 L. M. Liz-Marzan, M. Giersig and P. Mulvaney, *Langmuir*, 1996, **12**, 4329.
8 L. M. Liz-Marzan, M. Giersig and P. Mulvaney, *Chem. Commun.*, 1996, 731.
9 C. Graf and A. V. Blaaderen, *Langmuir*, 2002, **18**, 524.
10 K. Dick, T. Dhanasekaran, Z. Zang and M. D. Meisel, *J. Am. Chem. Soc.*, 2002, **124**, 2312.
11 A. Sreekumaran Nair, R. T. Tom, V. Suryanarayanan and T. Pradeep, *J. Mater. Chem.*, 2003, **13**, 297.
12 A. Imhof, M. Megens, J. J. Engelberts, D. T. N. de Lang, R. Sprik and W. L. Vos, *J. Phys. Chem. B*, 1999, **103**, 1408.
13 D. S. Koktysh, X. Liang, B. Yun, I. Pastoriza-Santos, R. L. Matts, M. Giersig, C. Serra-Rodriguez, L. M. Liz-Marzan and A. Kotov, *Adv. Funct. Mater.*, 2002, **12**, 255.
14 M. Bruchez, M. Moronne, P. Gin, S. Weiss and A. P. Alivisatos, *Science*, 1998, **281**, 2013.
15 D. Gerion, F. Pinaud, S. C. Williams, W. J. Parak, D. Zanchet, S. Weiss and A. P. Alivisatos, *J. Phys. Chem. B*, 2001, **105**, 8861.
16 D. Gerion, W. J. Parak, S. C. Williams, D. Zanchet, C. M. Michael and A. P. Alivisatos, *J. Am. Chem. Soc.*, 2002, **124**, 7070.
17 K. Kalyanasundaram and M. Gratzel, in *Optoelectronic Properties of Inorganic Solids*, ed. D. M. Roundhill and J. P. Fackler, Jr., Plenum Press, New York, 1999, p. **169**.
18 S. Wang, D.-G. Choi and S. -M. Yang, *Adv. Mater.*, 2002, **14**, 1311.
19 R. Philip, G. R. Kumar, N. Sandhyarani and T. Pradeep, *Phys. Rev. B*, 2000, **62**, 1360.
20 R. T. Tom, A. Sreekumaran Nair, N. Singh, M. Aslam, C. L. Nagendra, R. Philip, K. Vijayamohanan and T. Pradeep, *Langmuir*, 2003, **19**, 3439.
21 V. Eswaranand and T. Pradeep, *J. Mater. Chem.*, 2002, **12**, 2421.
22 I. Pastoriza-Santos and L. M. Liz-Marzan, *Langmuir*, 1999, **15**, 948.
23 Reduction of $AuCl_4^-$ has been reported recently. See, I. Pastoriza-Santos and L. M. Liz-Marzan, *Langmuir*, 2002, **18**, 2888.
24 J. Y. Yu, S. Schreiner and L. Vaska, *Inorg. Chim. Acta*, 1990, **70**, 145.
25 A. Sreekumaran Nair, T. Pradeep and I. MacLaren, *J. Mater. Chem.*, 2004, **14**, 857.
26 A. Sreekumaran Nair and T. Pradeep, *Curr. Sci.*, 2003, **84**, 1560.
27 (*a*) L. Valdez-Castro, J. Mendez-Vivar and R. Mendoza-Serna, *J. Porous Mater.*, 2001, **8**, 303; (*b*) M. Epifani, C. Giannini, L. Tapfer and L. Vasanelli, *J. Am. Ceram. Soc.*, 2000, **83**, 2385; (*c*) M. F. Wilhelm, T. I. Carsten, W. Michael and K. H. Chan, *Adv. Mater.*, 1993, **5**, 726.
28 Md. K. Nazeeruddin, S. M. Zakeerddin, R. Humphry-Baker, M. Jirousek, P. Liska, N. Vlachopoulos, V. Shklover, F. Christian-H and M. Gratzel, *Inorg.Chem.*, 1999, **38**, 6298.
29 B. V. Enustun and J. Turkevich, *J. Am. Chem. Soc.*, 1963, **85**, 3317.
30 N. K. Chaki, S. G. Sudrik, H. R. Sonawane and K. Vijayamohanan, *Chem. Commun.*, 2002, 76.
31 M. Aslam, N. K. Chaki, I. S. Mulla and K. Vijayamohanan, *Appl. Surf. Sci.*, 2001, **182**, 338.
32 D. A. J. Rand, *Proc .R. Aust. Chem. Inst.*, 1974, **41**, 43.